Article

Structure and Supersaturation of Highly Concentrated Solutions of Buckyball in 1-Butyl-3-Methylimidazolium Tetrafluoroborate

Eudes Eterno Fileti, and Vitaly V. Chaban

Just Accepted

Structure and Supersaturation of Highly Concentrated Solutions of

Buckyball in 1-Butyl-3-Methylimidazolium Tetrafluoroborate

Eudes Eterno Fileti[1] and Vitaly V. Chaban[2]*

[1] Instituto de Ciência e Tecnologia, Universidade Federal de São Paulo, 12231-280, São José dos Campos, SP, Brazil

[2] MEMPHYS — Center for Biomembrane Physics, Syddansk Universitet, Odense M, 5230, Kingdom of Denmark

Abstract. Solubilization of fullerenes is of high interest because of their wide usage in both fundamental research and numerous applications. This paper reports molecular dynamics (MD) simulations of saturated and supersaturated solutions of C_{60} in 1-butyl-3-methylimidazolium tetrafluoroborate, $[C_4C_1IM][BF_4]$, room-temperature ionic liquid (RTIL). The simulations cover a wide range of temperatures between 280 and 500 K at ambient pressure. Unlike in simpler solvents, C_{60} in $[C_4C_1IM][BF_4]$ forms highly supersaturated solutions, whose internal arrangement remains unaltered during nearly a microsecond-long real-time dynamics. The ion-molecular structure patterns in saturated and supersaturated solutions are distinguished in terms of radial distribution functions and cluster analysis of the solute particles. Cation separated solute pair is found to be a common structure in both saturated and supersaturated solutions. This observation suggests that imidazolium cation plays an important role in the successful dispersion of C_{60} molecules. Anticipated practical applications of the observed phenomenon are briefly discussed.

Keywords: fullerene, ionic liquid, supersaturation, solution, molecular dynamics.

---

* Email for correspondence: fileti@gmail.com; vvchaban@gmail.com; chaban@sdu.dk

Introduction

Fullerene C_{60} is one of the most studied molecules of all times.[1] The research interest to C_{60} comes from a wide horizon of potential applications in diverse areas,[2-7] such as electronics, biomedicine, and cosmetics industry.[8] For most applications, C_{60} needs to be solubilized. For example, industrial applications of light fullerenes require their fine dispersion in organic and lipophilic media. In turn, biomedical applications anticipate stable aqueous phases containing fullerenes.[9]

The buckyball, C_{60}, is a notably hydrophobic molecule. Its solubility in water amounts to less than 10^{-12} g L^{-1}. Therefore, one can think of C_{60} as a virtually insoluble particle in water. A systematic investigation of 47 solvents has revealed that the most suitable liquids for the solubilization of C_{60} exhibit a similar set of physical properties compared to fullerenes: high refractive index, dielectric constant of ca. 4 and large molecular volume.[10] A large variety of common solvents and their mixtures have been probed to obtain real solutions of C_{60}, C_{70}, and some higher fullerenes.[11-13] More or less concentrated solutions can be achieved in some solvents of low polarity, such as aromatic hydrocarbons and their halogen derivatives. For instance, solubility of C_{60} in benzene equals to 1.50 g L^{-1},[14] 2.40 g L^{-1} in toluene,[15] 2.60 g L^{-1} in ethylbenzene.[14] All referenced measurements have been conducted at 298 K.

As organic solvents which are suitable for the solubilization of C_{60} are often not appropriate to introduce exogenous compounds into biological systems, research on the solubility of C_{60} remains a challenging field.[16,17] Fullerene partitioning and dispersion in lipid membranes have been investigated by both experimental and computational techniques.[16,17] Partitioning of C_{60} into lipid membranes, demonstrating a competitive thermodynamic affinity towards fullerenes, has been recorded. However, fullerene dispersion within those membranes is still elusive.[10] We have recently proposed to disperse C_{60} in room-temperature ionic liquids (RTIL). We investigated physical chemical

properties of the concentrated solutions of C_{60} in $[C_4C_1IM][BF_4]$ RTIL using classical molecular dynamics simulations and found that the solubility of C_{60} in this RTIL at slightly elevated temperatures (T > 310 K) is higher than in most previously investigated solvents due to certain amount of charge transfer between the solute and the solvent.[18]

If a solution contains more solute than could be dissolved by the solvent under normal conditions (in the state of free energy minimum), it can still remain stable over a significant amount of time. Such solutions are termed supersaturated ones. Their usage in real-world applications and natural systems is quite extensive. Supersaturated solutions play a vital role in chemistry and physics of materials.[19-23] For instance, they are widely used in production of artificial crystals and solvation of manifold minerals.[24,25] A highly promising direction is the use of supersaturated solutions to facilitate transport of drug particles into the cell interior.[19,26,27]

Within this paper, we compare supersaturated and saturated solutions of C_{60} in $[C_4C_1IM][BF_4]$ RTIL at room (300 K) and somewhat elevated temperatures (340-360 K) using atomistic-precision molecular dynamics (MD) simulations. The solubility of C_{60} in $[C_4C_1IM][BF_4]$ was calculated at 280, 300, 320, 340, 360, 380, 400, 450, and 500 K. We underline differences between supersaturated C_{60} solutions in the selected RTIL and in water. In the latter, supersaturation is unequivocally prohibited for thermodynamic reasons. As an instance of metastable state, supersaturated solutions provide a specific challenge for computer simulation techniques based on statistical mechanics. We provide a brief discussion of the related methodological issues.

Methodology

To investigate the thermal impact in the dissolution of fullerene C_{60} in $[C_4C_1IM][BF_4]$ ionic liquid, nine simulations were performed at temperatures ranging from 280 to 500 K. Three separate simulations of 800 ns each were employed to check the

stability of supersaturated solutions at room temperature with different concentration of C_{60} (10, 20, and 30 molecules per 500 ion pairs). Additionally, the saturated solution was cooled from 400 K down to 300 K during 500 ns that corresponds to a temperature reduction rate of 0.2 K ns^{-1}. The goal of this simulation was to observe gradual decrease of supersaturation, as the solubility of buckyball in $[C_4C_1IM][BF_4]$ is in inverse proportion to temperature. The rate of aggregation of C_{60} in alternative environment was estimated based on MD simulation during 10 ns in water at ambient conditions. The initial cells to model the supersaturated solutions were composed of 10-30 C_{60} molecules dispersed or aggregated within 500 ion pairs of $[C_4C_1IM]^+/[BF_4]^-$. The simulated systems, therefore, contain ca. 16 thousands of interaction centers. The set of selected snapshots of the simulation boxes is represented in Figure 1. The details of the performed simulations are summarized in Table 1.

Table 1: List of the discussed systems

#	N(solvent)	N(C_{60})	Time*, ns	Temperature, K	Starting point
1-9		30	50	280, 300, 320, 340, 360, 380, 400, 450, 500	Single cluster of 30 C_{60}
10		30	800	300	
11	500	20	800	300	Dispersed C_{60}'s at 500 K
12	$[C_4C_1IM][BF_4]$	10	800	300	
13-15		30	220	340, 350, 360	
16		30	500	Cooling from 400 to 300 (dT/dt=0.2 K/ns)	Dispersed C_{60}'s at 400 K
17	4631 H_2O	30	10	300	Artificially dispersed C_{60}'s

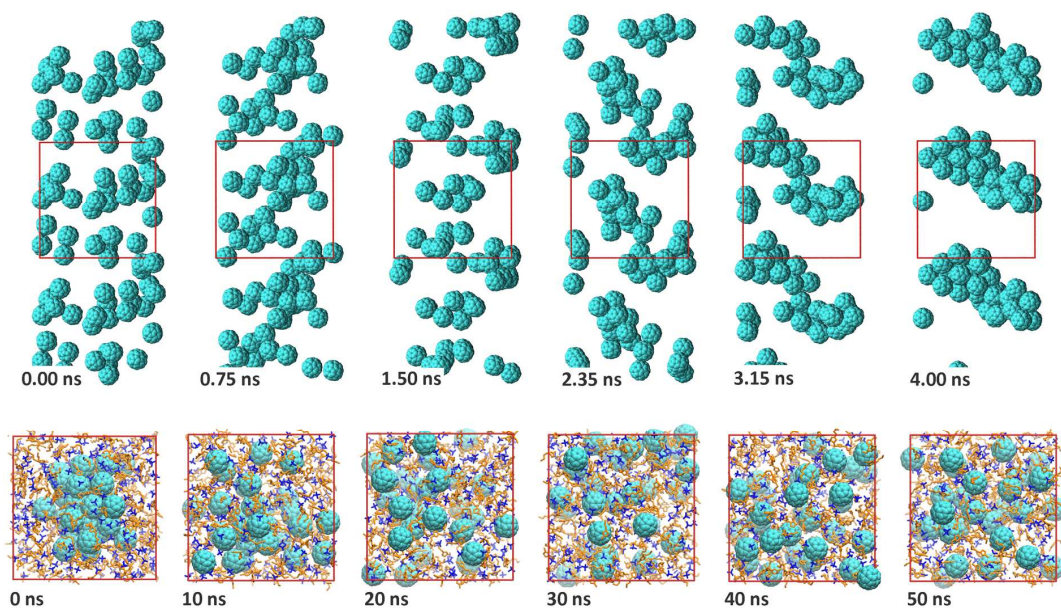* All sampling times correspond to the total duration of the MD runs.

Figure 1. The simulated systems: (top) time-line of fullerene aggregation in water (water omitted for clarity); (bottom) time-line of fullerene dispersion in ionic liquid. The box boundaries are depicted by red lines. Top and bottom periodic images are depicted in case of aggregation.

The parameters proposed by Rivelino et. al.[28] for C_{60} were initially applied. The interactions between fullerene and RTIL were refined as justified in our previous work.[18] The fullerene force field model treats each uncharged carbon atom by means of pairwise Lennard-Jones (12,6) equation. This force field has proved its reliability for the investigation of structure, dynamics, and solubility of C_{60} in ionic, organic and aqueous environments.[18,29-31]

The ionic liquid, $[C_4C_1IM][BF_4]$, was simulated using the empirical potential utilizing reduced charges by Chaban et. al.[32] TIP3P model was used to describe water molecule.[33] Note that RTIL and water were simulated only separately from one another. Therefore, justification of the compatibility of the corresponding parameters is not

required. The total potential energy of the constructed simulation cells was minimized

following a short equilibration at room temperature. Various durations of production

simulation stage were used, as dictated by the goal of the particular simulation (Table 1).

For instance, simulation of dissolution required only 50 ns to get all necessary physical

insights. In turn, simulations of the supersaturated states were conducted for a longer time

to observe the dynamics of particle aggregation. All systems were maintained at the

requested temperature (see Table 1 for details) and pressure (1 bar) using velocity rescaling

thermostat[34] and isotropic Parrinello-Rahman[35] barostat. The time constants of 1.0 and 4.0

were applied to couple temperature and pressure, respectively. The cut-off distance of 1.2

nm for Lennard-Jones potential was employed in conjunction with the shifted force

modification between 1.1 and 1.2 nm. The electrostatic interactions were computed using

direct pairwise Coulomb potential at the separations smaller than 1.4 nm and using

Particle-Mesh-Ewald scheme[36] for all distances beyond the cut-off. The neighbor list was

updated every 0.02 ps within 1.4 nm. All simulations of molecular dynamics trajectories

were performed using the GROMACS 4.5 program.[37,38]

Results and Discussion

Fullerene C_{60} exhibits a surprisingly good solubility in $[C_4C_1IM][BF_4]$ ionic liquid

(Figure 2). Although no buckyballs are found in the liquid phase at 280-300 K (zero

solubility), concentration of the solutions uniformly increases at higher temperatures. The

content of 50 grams of C_{60} per one liter of solution can be obtained at 320 K, increasing by

almost four times (190 g L^{-1}), when the system is heated up to 380 K. The validity of

solubilities at even higher temperatures is unclear, as $[C_4C_1IM][BF_4]$ is believed to start

reactive decomposition upon further heating. The decomposition mechanism includes a

strong interaction of $[C_4C_1IM][BF_4]$ with water, which is absent in our theoretical

investigation, but is omnipresent in laboratory and industrial samples of this RTIL due to

its remarkable hygroscopicity.[39] The speed of solute dispersion in a liquid is clearly

dependent on temperature, exceeding one C_{60} per nanosecond at 400-450 K. It should be

noted that dispersion speed of any species is directly proportional to the solid/liquid

interface surface area. Thus, the presented numbers can be plainly extrapolated to the

macroscopic quantities of the solute. Solubility versus temperature is summarized in
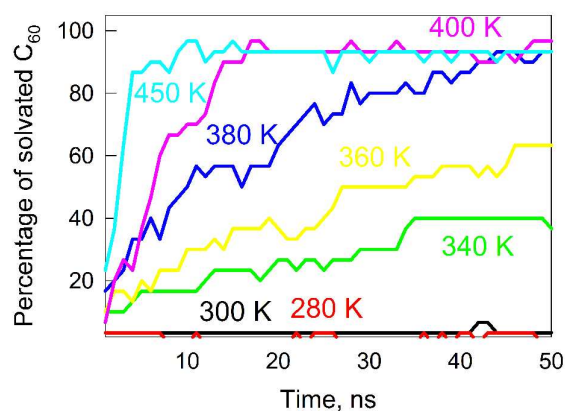
Figure S1 of Supplementary Information.

Figure 2. Percentage of dispersed fullerenes C_{60} versus simulated time at fixed

temperature. The data are derived from systems (1-9), whose starting point is a solid/liquid

interface. See designations in the plot. While solid phase remains unaltered at 280-300 K

(in agreement with most recent experiments), at higher temperatures (320-450 K) the

interface quickly evolves finishing with a homogeneous state (380-450 K).

The systems, where complete dissolution was observed, were immediately cooled

down to 300 K. The additional trajectory of the system spontaneous evolution was

recorded. Figure 3 depicts concentrations of supersaturated solutions, containing 10, 20,

and 30 C_{60} molecules. The system, where supersaturated state is not stable, would

gradually decrease concentration, until it approaches the corresponding saturated state (at

given temperature and pressure). Note, that saturated state of C_{60} in $[C_4C_1IM][BF_4]$ RTIL

exhibits negligible solubility at 300 K (Figure 2). This theoretical result is in complete

agreement with the recent experimental data.[40] However, none of the simulated supersaturated solution decreased its concentration during 800 ns of spontaneous molecular dynamics. Formation and destruction of C_{60} dimers and trimers was observed during simulations (Figure 3), thus formally decreasing or increasing the amount of "dissolved" fullerenes. Nevertheless, no systematic solid/liquid phase separation was found. It is in contrast to many other probed solvents, where aggregation of C_{60} takes place within a few nanoseconds. As an example, Supplementary Information provides a dynamics of desupersaturation of buckyball solution in water at ambient conditions (Figure S2). Based on our computational results, $[C_4C_1IM][BF_4]$ provides an excellent environment for preparation of supersaturated solutions of C_{60}. Such solutions are expected to become of importance for numerous applications of fullerenes, such as drug delivery vehicles, antioxidant functionality, anti-HIV treatment, etc.[41] All these applications cannot make a proper use of aggregated solid-phase fullerenes, while the observed solutions must drastically boost their efficacy.
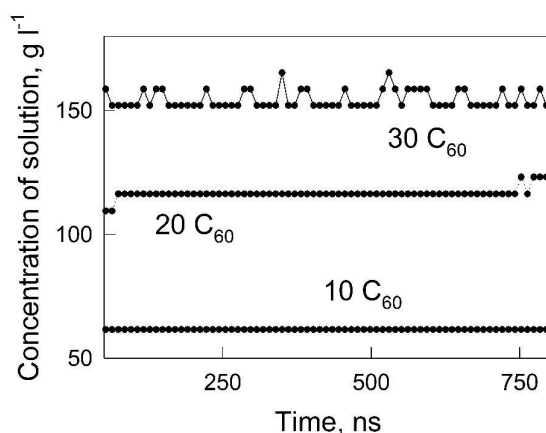

Figure 3. Concentrations of supersaturated solutions of C_{60} in $[C_4C_1IM][BF_4]$ as a function of simulated time at 300 K. The data are derived from systems (10-12), whose starting points are the configurations spontaneously obtained at 500 K. Note that C_{60} exhibits negligible solubility in $[C_4C_1IM][BF_4]$ at 300 K. Therefore, these solutions are supersaturated by definition.

The structure of the three supersaturated solutions is characterized in terms of pair radial distribution functions (Figure 4). RDFs computed between centers-of-mass of neighboring C_{60} molecules indicate a clearly defined maximum at 1.05 nm, which should be ascribed to a contact fullerene pair, i.e. a dimer. Indeed, the experimentally known van der Waals radius of C_{60} equals to 0.55 nm. Interestingly, only the two systems, in particular those containing 20 and 30 C_{60} molecules, form contact solute pairs, while the system with lower solute concentration, 10 C_{60}, contains none. As should be expected, the system with higher concentration and, hence, supersaturation, exhibits a higher first peak. The second peak, which is somewhat higher than the first one, is observed at 1.35 nm. This maximum is nearly of the same height in all systems, corresponding to the solvent separated C_{60} pair. The difference between the first and the second peaks ideally corresponds to the van der Waals diameters of carbon and nitrogen atoms (ca. 0.30 nm). Therefore, we hypothesize that neighboring C_{60} particles are separated by the imidazole ring. The proof of this hypothesis is provided in Figure 5 by means of three-dimensional distribution of spatial probabilities. Cation separated solute pair appears to be a stable formation in supersaturated solutions. The fraction of such structural patterns in room-temperature supersaturated fullerene solutions is the highest one.
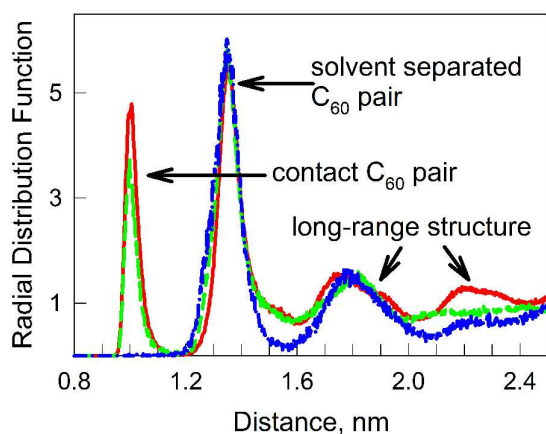
Figure 4. Radial distribution functions computed between centers-of-mass of neighboring fullerene molecules in systems (10-12) at 300 K. Red solid line corresponds to 30 C_{60} in 500 $[C_4C_1IM][BF_4]$, green dashed line corresponds to 20 C_{60} per system, and blue dash-dotted line corresponds to 10 C_{60} per system, whereas the number of ion pairs (500) is the same in all systems. All three RDFs feature a well-ordered long-range structure of fullerene molecules in the prepared solutions.
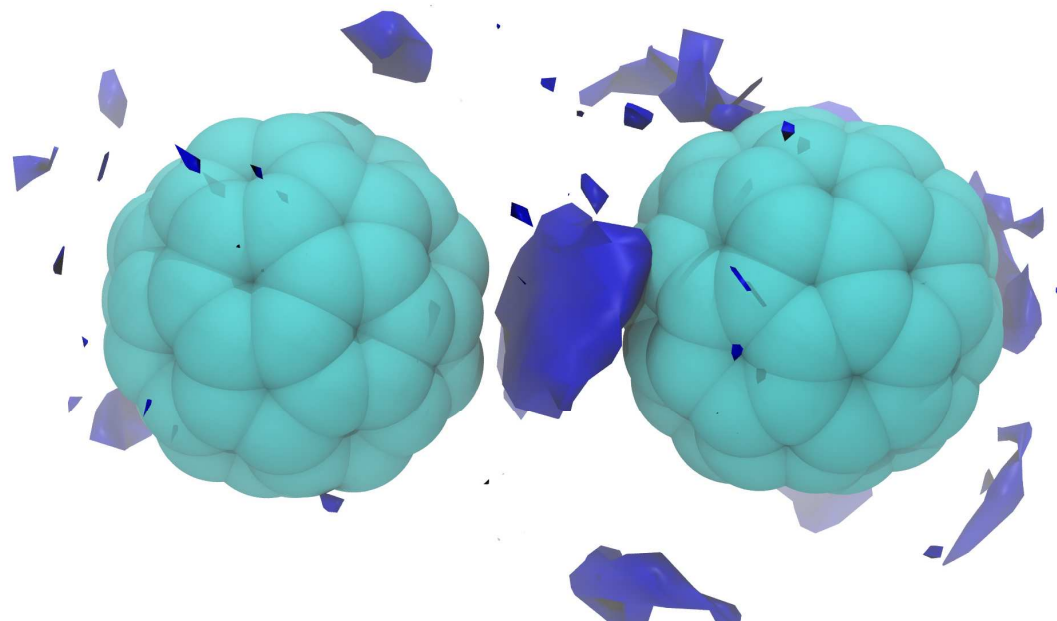
Figure 5. Spatial distribution function of $[C_4C_1IM]$ cation (in blue) in region between two C_{60} molecules. The surface has been drawn at an isovalue of 3.4 for a selected fullerene pair in the supersaturated solution at 340K.

The anions are concentrated around cationic rings in order to compensate an excess positive charge. However, they do not play a principal role in the dispersion of buckyballs. If they did, the difference between the first peak and the second peak would have been roughly 0.4 nm, which is the diameter of tetrafluoroborate anion. The diameter of fluorine atom is 0.27 nm and fluorine-boron bond length in BF_4^- is 0.143 nm, while the entire structure adheres tetrahedral shape. These observations, among other things, suggest that other imidazolium-based RTILs exhibit a similar affinity towards C_{60}, in spite of the

anionic species they contain. Additional two maxima are located at distance separations of 1.8 and 2.2 nm. The latter one is present essentially only in the most concentrated solution. Four peaks in the pair radial distribution are not characteristic for the liquid state of matter, suggesting that the investigated system is rather in the glassy state. Unfortunately, precise computation of shear viscosity in this system appeared problematic because of insufficient sampling. The value estimated from self-diffusion constant, following Stokes-Einstein relation, is ca. 1000 cP, being 10 times higher than the shear viscosity of pure $[C_4C_1IM][BF_4]$ at the same temperature.[32]

The glassy state of the supersaturated C_{60} solution in $[C_4C_1IM][BF_4]$ can be validated using information about diffusion regimes (Figure 6). First, at short times, t < 50 ps, a ballistic motion prevails. Upon ballistic motion, MSD evolves proportionally to t^2, since the motion of the particle (either C_{60} or RTIL) is not yet affected by the presence of other molecules or atoms surrounding it. Second, between t = 50 ps and a few nanoseconds all motions are slowed down. This is because the particles are starting to collide with their neighbors, thus basically rattling in the cage formed by the surrounding molecules. The ions and C_{60}s participating in the formation of this cage are themselves located in the cages. The molecules, afterwards, succeed to escape the cage starting a diffusive regime, where MSD is proportional to time. The transition from the cage regime to the diffusive regime is gradual. There is no sharp transition time. For instance, diffusion constants obtained from the cage regime are only ca. 20% smaller than those from diffusive regime. Demonstration of the three stages of glassy dynamics supports our hypothesis that was deduced from the analysis of RDF. The hypothesis is also supported by a notably high shear viscosity.
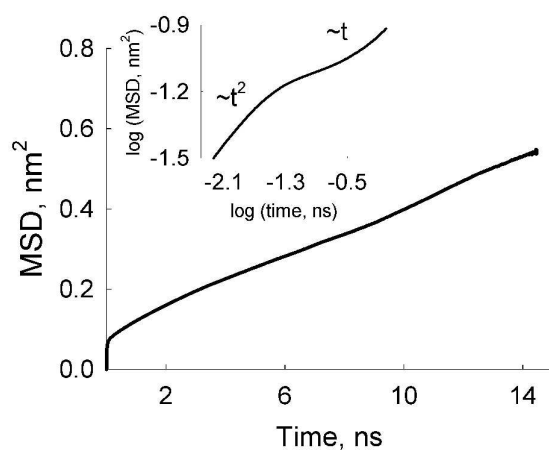
Figure 6. Mean-square displacements (MSD) of all particles versus time (system 10). The MSD is characteristic to glassy state systems exhibiting different diffusion regimes. Inset: MSD evolution during the first picoseconds using the log (MSD)-log(time) scale.
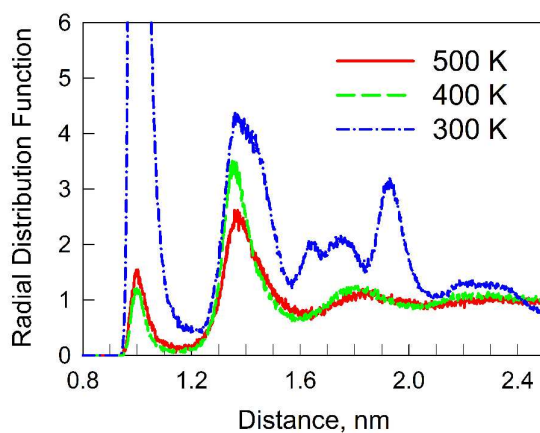
Figure 7. Radial distribution functions computed between centers-of-mass of neighboring fullerene molecules in saturated solutions at 300, 400, and 500 K. See systems (1-9) in Table 1 for details. While RDF at 300 K is characteristic for solid phase of C_{60}, systems at 400 and 500 K exhibit homogeneous phase with two well-defined peaks (at ca. 1.05 and 1.35 nm) between fullerene centers-of-mass.

The structure of C_{60} in supersaturated solutions (Figure 4) was directly compared with the structure of saturated solutions (Figure 7). As the liquid/solid interface remains stable at 300 K, the corresponding C_{60}-C_{60} RDF reflects the structure of the solid phase

only. Two maxima are present at 400 and 500 K, one of which is a contact C_{60} pair, while another reflects a solvent separated C_{60} pair. Unlike in supersaturated solutions, long-range structure in saturated solutions is marginal. The common feature of both kinds of the $C_{60}/[C_4C_1IM][BF_4]$ solution is that the pattern containing a solvent separated C_{60} pair is more ordered than the pattern containing a contact C_{60} pair. The buckyballs interact primarily through relatively weak van der Waals forces. The ions of imidazolium RTIL interact mainly through stronger electrostatic forces. Therefore, these substances alone exhibit quite different phase diagrams. While quite a few buckyballs sublimate at 400-500 K at atmospheric pressure establishing solid/vapor equilibrium, RTIL remains in the liquid state. Hence, $[C_4C_1IM][BF_4]$ possesses a more ordered internal ionic structure than fullerene C_{60} does. Imidazolium-based cations act like a glue sticking significantly mobile C_{60} particles at the elevated temperatures, whereas C_{60} contact pairs (dimers) are relatively unstable. The motion of C_{60} contact pairs is poorly correlated at the temperatures above 340 K. This feature can, upon necessity, be quantified by considering RTIL-C_{60}/vapor interface and estimating the extent to which RTIL interferes sublimation of C_{60}.

Since the supersaturated state observed at 300 K resembles a glassy system, we have extended the simulations to higher temperatures, 340, 350, 360 K (systems 13-15, respectively). Figure 8 presents solubility as a function of time. Although the formation of small C_{60} aggregates is observed during spontaneous dynamics, dispersed fullerenes do not aggregate into larger structures. The derived solubilities at 340-360 K range between 170-190 g L^{-1}, which constitutes a very significant value compared to other known solvents. Since the solubility in Figure 6 is expressed per unit of volume, the supersaturation is somewhat higher at lower temperature (340 K). The thermal extension/contraction of the systems explains this difference.
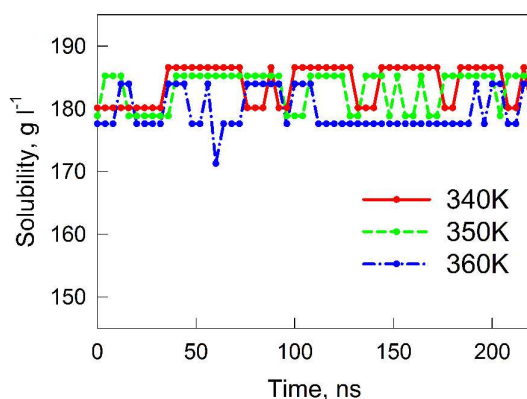
Figure 8. Solubility of supersaturated C_{60} solutions in $[C_4C_1IM][BF_4]$ versus simulated time at 340 (red solid line), 350 (green dashed line), and 360 K (blue dash-dotted line). The data are derived from systems (13-15).

As compared to supersaturated solutions at room temperature (Figure 4), the ones at 340-360 K (Figure 9) exhibit insignificant long-range structure (only a peak at 1.8 nm exists). The first peak, standing for the contact fullerene pair in solution, is of tiny height, whereas the primary local structure pattern is exemplified by the cation separated solute pair, at 1.35-1.40 nm. Over 96% of all buckyballs in supersaturated solutions exist as solvated solute particles, i.e. form a real solution (Figure 10). Less than 3% C_{60} exists in the form of dimers, while only 0.1-0.5% C_{60} is involved in trimers. Temperature does not play a significant role in case of cluster size distributions.

Figure 9. Radial distribution functions computed between centers-of-mass of neighboring C_{60} molecules in saturated solutions at 340, 350, and 360 K. See systems (13-15) in Table 1 for details.

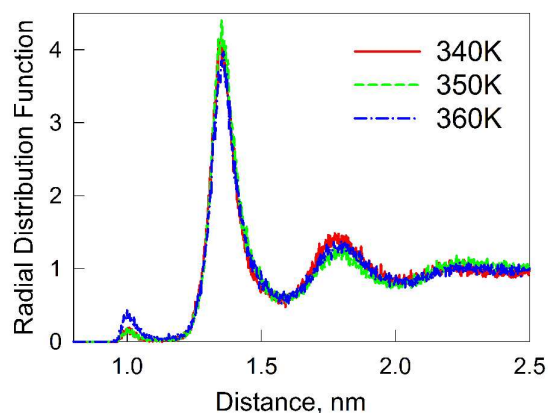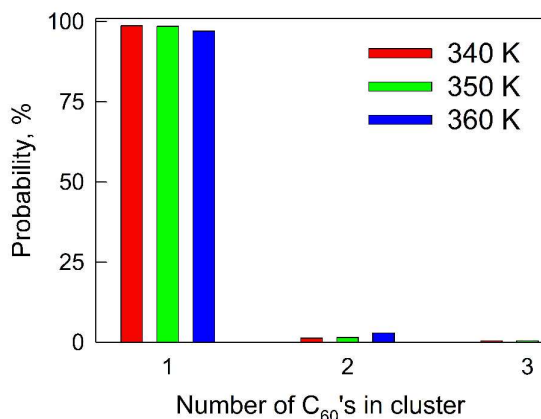Figure 10. The recorded aggregates containing C_{60} fullerenes in systems (13-15) at 340-360 K averaged over the whole trajectory length. The error bars do not exceed 1%.

As follows from the above discussion, the supersaturated solutions of fullerene C_{60} can be obtained by a preparation of highly saturated solutions in $[C_4C_1IM][BF_4]$ and subsequent fast cooling down to 300-340 K. In order to estimate whether the speed of cooling influences stability of the considered solutions, we simulated gradual cooling of system (16) from 400 to 300 K during 500 ns. The obtained plot of solubility versus simulated time is identical to those in Figures 3 and 6. Slower cooling may, of course, change the qualitative observations, although is virtually prohibited by the corresponding computational cost. The subsequent experimental investigation is, therefore, deemed necessary. The stability of supersaturated solutions of C_{60} in $[C_4C_1IM][BF_4]$ cannot be explained exclusively by a slow self-diffusion of fullerenes in these systems. The average diffusion constants at 340, 350, and 360 K equal to 7, 8, and 9 ($\times 10^{-11}$ m^2 s^{-1}). The listed values were derived from the mean-squared displacements of atoms in the corresponding

systems (Table 1) under an assumption that these systems are in the equilibrium state. The supersaturated solution is, rigorously speaking, a metastable state. Therefore, each particle, in average, shifts by 10 nm per microsecond of simulated dynamics. Since the linear size of the simulated systems is ca. 6x6x6 nm (the exact box side length depends on thermal expansion/contraction), the particles spontaneously diffuse across more than a half of the box. Such mobility of the solute, in combination with such simulation times, are enough for aggregation to take place, provided there is a driving force (free energy gradient) among the states. Compare, all 30 C_{60} molecules distributed in water aggregate in 2 ns in the box of the same size and room temperature (system 17), while self-diffusion constant of the solute in that system equals to ca. 1×10^{-9} m^2 s^{-1}.

Supersaturated solution represents a metastable state, whose numerical simulation is always complicated by the limited available length and time scales. By definition, the simulated supersaturated solutions will self-transform into saturated solutions, although the necessary time may be seconds, minutes or even years. Numerical simulations with atomistic precision can provide hints on the possible stability or instability of supersaturated states in given systems. For instance, the supersaturated solutions of C_{60} in water (Figure S2), dimethyl sulfoxide and chloroform (not reported in this paper) are clearly possible only during hundreds of picoseconds. That is, these solutions cannot be used for applications. However, simulations are unable to precisely determine the stability time for such solutions, provided that available sampling time is inferior to the sought stability time. Currently certain works exist, mainly devoted to inorganic salts in water, demonstrating that adequate description of the investigated phenomenon is possible within the scope of atomistic simulations.[42] The relatively fast aggregation of C_{60} in water (Figure S2) shows that supersaturated solutions of C_{60} in this solvent are highly unstable and, therefore, their existence over macroscopic times is thermodynamically forbidden.

The numerical results and qualitative observations presented here must be understood as a prediction and motivation for an experimental implementation of the systems considered in our computer modeling. Should the discussed solutions confirm their stability over significant time scales, they will promote a large number of real-world applications of fullerenes.

Conclusions

The present paper introduces the first simulation attempt of supersaturated C_{60} solutions in the $[C_4C_1IM][BF_4]$ RTIL over a wide temperature range. The highly concentrated supersaturated solutions were found stable in nearly microsecond-long molecular dynamics simulations. The structure of supersaturated solutions was numerically characterized and compared with the saturated solutions of the same solute-solvent composition. The stable cation separated solute-solute pair was found in solutions. The proposed systems are anticipated to find a niche of applications in the biomedical field and possibly in materials science.[41]

Since $[C_4C_1IM][BF_4]$ RTIL is well miscible with water, its affinity to fullerenes must be further exploited in RTIL/water/C_{60} systems, where C_{60} is coated by $[C_4C_1IM][BF_4]$ in order to create water-soluble fullerenes. Therefore, theoretical and experimental investigation of fullerene solvation in the RTIL/water mixtures is of significant interest and is deemed urgent for fullerene science.

Acknowledgments

Supporting Information Available

Figures S1 and S2 referenced in the manuscript can be found in Supporting Information. This information is available free of charge via the Internet at http://pubs.acs.org.

REFERENCES

(1)   Abraham, M. H. Thermodynamics of Solution of Homologous Series of Solutes in Water. *J. Chem. Soc. Faraday Trans.* **1984**, *80*, 153.

(2)   Su, G. X.; Czader, A.; Homouz, D.; Bernardes, G.; Mateen, S.; Cheung, M. S. Multiscale Simulation on a Light-Harvesting Molecular Triad. *J. Phys. Chem. B* **2012**, *116*, 8460-8473.

(3)   Tezuka, N.; Umeyama, T.; Matano, Y.; Shishido, T.; Kawasaki, M.; Nishi, M.; Hirao, K.; Lehtivuori, H.; Ikachenko, N. V.; Lemmetyinen, H.et al. Good Solvent Effects of C-70 Cluster Formations and Their Electron-Transporting and Photoelectrochemical Properties. *J. Phys. Chem. B* **2010**, *114*, 14287-14297.

(4)   Li, H.; Hao, J. Phase Behavior of Salt-Free Catanionic Surfactant Aqueous Solutions with Fullerene C-60 Solubilized. *J. Phys. Chem. B* **2007**, *111*, 7719-7724.

(5)   Jarzab, D.; Cordella, F.; Lenes, M.; Kooistra, F. B.; Blom, P. W. M.; Hummelen, J. C.; Loi, M. A. Charge Transfer Dynamics in Polymer-Fullerene Blends for Efficient Solar Cells. *J. Phys. Chem. B* **2009**, *113*, 16513-16517.

(6)   Pieta, P.; Grodzka, E.; Winkler, K.; Warczak, M.; Sadkowski, A.; Zukowska, G. Z.; Venukadasula, G. M.; D'Souza, F.; Kutner, W. Conductive, Capacitive, and Viscoelastic Properties of a New Composite of the C-60-Pd Conducting Polymer and Single-Wall Carbon Nanotubes. *J. Phys. Chem. B* **2009**, *113*, 6682-6691.

(7)   Raffaini, G.; Ganazzoli, F. A Molecular Dynamics Study of the Inclusion Complexes of C-60 with Some Cyclodextrins. *J. Phys. Chem. B* **2010**, *114*, 7133-7139.

(8)   *Fullerenes: Nanochemistry, Nanomagnetism, Nanomedicine, Nanophotonics*; Sheka, E., Ed.; CRC Press: New York, **2011**.

(9)   Bakry, R.; Vallant, R. M.; Haq, M. N.; Rainer, M.; Szabo, S.; Huck, C. W.; Bonn, G. K. Medicinal Applications of Fullerenes. *Int J Nanomedicine* **2007**, *2*, 639-649.

(10)   Ruoff, R. S.; Tse, D. S.; Malhotra, R.; Lorents, D. C. Solubility of Fullerene (C60) in a Variety of Solvents. *J. Phys. Chem.* **1993**, *13*, 3379–3383.

(11)   Semenov, K. N.; Charykov, N. A. Temperature Dependence of Solubility of Individual Light Fullerenes and Industrial Fullerene Mixture in 1-Chloronaphthalene and 1-Bromonaphthalene. . *J Chem Eng Data* **2010**, *55*, 2373-2378.

(12)   Semenov, K. N.; Charykov, N. A.; Keskinov, V. A.; Piartman, A. K.; Blokhin, A. A.; Kopyrin, A. A. Solubility of Light Fullerenes in Organic Solvents. *J Chem Eng Data* **2010**, *55*, 13-36.

(13)   Petrossyan, N. O. Fullerenes in Molecular Liquids. Solutions in "Good" Solvents: Another View. *J. Mol. Liq.* **2011**, *161*, 1-12.

(14)   Scrivens, W. A.; Tour, J. M. Potent Solvents for C60 and Their Utility for the Rapid Acquisition of C13 NMR Data for Fullerenes. *J Chem Soc Chem Comm* **1993**, 1207-1209.

(15)   Talukdar, S.; Pradhan, P.; Banerji, A. Electron Donor-Acceptor Interactions of C60 with N- and Pi-Donors: A Rational Approach Towards Its Solubility. *Fullerene Sci Technol* **1997**, *5*, 547-557.

(16)   Zhang, S.; Mu, Y.; Zhang, J.; Xu, W. Effect of Self-Assembly of Fullerene Nano-Particles on Lipid Membrane. *PloS ONE* **2013,** DOI: 10.1371/journal.pone.0077436.g009.

(17)   Rossi, G.; Barnoud, J.; Monticelli, L. Partitioning and Solubility of C60 Fullerene in Lipid Membranes. *Physica Scripta* **2013**, DOI: 10.1088/0031-8949/87/05/058503

1
2
3
4
5
6
7
8
9
10
11
12
13
14
15
16
17
18
19
20
21
22
23
24
25
26
27
28
29
30
31
32
33
34
35
36
37
38
39
40
41
42
43
44
45
46
47
48
49
50
51
52
53
54
55
56
57
58
59
60

(18)   Chaban, V. V.; Maciel, C.; Fileti, E. E. Does Like Dissolves Like Rule Hold for Fullerene and Ionic Liquids? *J. Chem. Sol.* **2014**, DOI: 10.1007/s10953-014-0155-6.

(19)   Higashi, K.; Yamamoto, K.; Pandey, M.; Mroue, K.; Moribe, K.; Yamamoto, K.; Ramamoorthy, A. Insights into Atomic-Level Interaction between Mefenamic Acid and Eudragit Epo in a Supersaturated Solution by High-Resolution Magic-Angle Spinning Nmr Spectroscopy. *Molecular Pharmaceutics* **2014**, *11*, 351-357.

(20)   Dietzsch, M.; Barz, M.; Schoeler, T.; Klassen, S.; Schreiber, M.; Susewind, M.; Loges, N.; Lang, M.; Hellmann, N.; Fritz, M. et al. Paa-Pamps Copolymers as an Efficient Tool to Control CaCO3 Scale Formation. *Langmuir* **2013**, *29*, 3080-3088.

(21)   Modi, S.; Xiang, T.-X.; Anderson, B. Enhanced Active Liposomal Loading of a Poorly Soluble Ionizable Drug Using Supersaturated Drug Solutions. *Journal of Controlled Release* **2012**, *162*, 330-339.

(22)   Liu, J.; Pancera, S.; Boyko, V.; Gummel, J.; Nayuk, R.; Huber, K. Impact of Sodium Polyacrylate on the Amorphous Calcium Carbonate Formation from Supersaturated Solution. *Langmuir* **2012**, *28*, 3593-3605.

(23)   Burton, R.; Ferrari, E.; Davey, R.; Finney, J.; Bowron, D. The Relationship between Solution Structure and Crystal Nucleation: A Neutron Scattering Study of Supersaturated Methanolic Solutions of Benzoic Acid. *J Phys. Chem. B* **2010**, *114*, 8807-8816.

(24)   Branislava, M. M.; Dragana, A. M.; Andrijana, A. Ž.; Mićo, M. M. Nongrowing Faces of Sodium Chlorate Crystals in Supersaturated Solution. *Crystal Growth & Design* **2014**, DOI: 10.1021/cg401162n.

(25)   Okada, I.; Namiki, Y.; Uchida, H.; Aizawa, M.; Itatani, K. MD Simulation of Crystal Growth of NaCl from Its Supersaturated Aqueous Solution. *J. Mol. Liq.* **2005**, *118*, *131-139*.

(26)   Yin, L.; Hillmyer, M. Preparation and Performance of Hydroxypropyl Methylcellulose Esters of Substituted Succinates for in Vitro Supersaturation of a Crystalline Hydrophobic Drug. *Molecular Pharmaceutics* **2014**, *11*, 175-185.

(27)   Kapoor, M.; Siegel, R. Prodrug/Enzyme Based Acceleration of Absorption of Hydrophobic Drugs: An in Vitro Study. *Molecular Pharmaceutics* **2013**, *10*, 3519-3524.

(28)   Rivelino, R.; Maniero, A. M.; Prudente, F. V.; Costa, L. S. Theoretical Calculations of the Structure and UV-Vis Absorption Spectra of Hydrated C-60 Fullerene. *Carbon* **2006**, *44*, 2925-2930.

(29)   Maciel, C.; Fileti, E. E.; Rivelino, R. Note on the Free Energy of Transfer of Fullerene C(60) Simulated by Using Classical Potentials. *J. Phys. Chem. B* **2009**, *113*, 7045-7048.

(30)   Colherinhas, G.; Fonseca, T. L.; Fileti, E. E. Theoretical Analysis of the Hydration of C(60) in Normal and Supercritical Conditions. *Carbon* **2011**, *49*, 187-192.

(31)   Fileti, E. E.; Maciel, C. Molecular Interactions between Fullerene C60 and Ionic Liquids. *Chem. Phys. Lett.* **2013**, *568*, 75-79.

(32)   Chaban, V. V.; Voroshylova, I. V.; Kalugin, O. N. A New Force Field Model for the Simulation of Transport Properties of Imidazolium-Based Ionic Liquids. *Phys. Chem. Chem. Phys.* **2011**, *13*, 7910–7920.

(33)   Berendsen, H. J. C.; Postma, J. P. M.; van Gunsteren, W. F.; Hermans, J. *In B. Pullman (Ed.), Intermolecular Forces*; Reidel: Dordrecht, 1981.

(34)   Bussi, G.; Donadio, D.; Parrinello, M. Canonical Sampling through Velocity Rescaling. *J. Chem. Phys.* **2007**, *126*, 014101-014108.

(35)   Parrinello, M.; Rahman, A. Polymorphic Transitions in Single Crystals: A New Molecular Dynamics Method. *J. Appl. Phys.* **1981**, *52,* 7182.

(36)   Darden, T.; York, D.; Pedersen, L. Particle Mesh Ewald: An N·Log(N) Method for Ewald Sums in Large Systems. *J. Chem. Phys.* **1993**, *98,* 10089.

(37)   Lindahl, E.; Hess, B.; van der Spoel, D. Gromacs 3.0: A Package for Molecular Simulation and Trajectory Analysis. *J. Molec. Modeling* **2001**, *7*, 306-317.

(38)   Berendsen, H. J. C.; van der Spoel, D.; van Drunen, R. Gromacs - a Message-Passing Parallel Molecular-Dynamics Implementation. *Computer Physics Communication* **1995**, *91*, 43.

(39)   Frolov; Endres; Castner; Jung; Taylor; Ouchi; Roling; Padua; Lopes, C.; MacFarlaneet al. General Discussion. *Faraday Discussions* **2012**, *154*, 313-333.

(40)   Martins, S.; Fedorov, A.; Afonso, C. A. M.; Baleizao, C.; Berberan-Santos, M. N. Fluorescence of Fullerene C-70 in Ionic Liquids. *Chemical Physics Letters* **2010**, *497*, 43-47.

(41)   Torres, V.; Posa, M.; Srdjenovic, B.; Simplicio, A. Solubilization of Fullerene C60 in Micellar Solutions of Different Solubilizers. *Colloids and Surfaces. B, Biointerfaces* **2011**, *82*, 46-53.

(42)   Aber, J. E.; Arnold, S.; Garetz, B. A.; Myerson, A. S. Strong DC Electric Field Applied to Supersaturated Aqueous Glycine Solution Induces Nucleation of the Gamma Polymorph. *Phys. Rev. Lett.* **2005**, *94*, 145503.

1
2
3
4
5
6
7
8
9
10
11
12
13
14
15
16
17
18
19
20
21
22
23
24
25
26
27
28
29
30
31
32
33
34
35
36
37
38
39
40
41
42
43
44
45
46
47
48
49
50
51
52
53
54
55
56
57
58
59
60

1
2
3
4
5
6
7
8
9
10
11
12
13
14
15
16
17
18
19
20
21
22
23
24
25
26
27
28
29
30
31
32
33
34
35
36
37
38
39
40
41
42
43
44
45
46
47
48
49
50
51
52
53
54
55
56
57
58
59
60

TOC Image

Cation separated C_{60} pair